Intra-seasonal variation of the Kuroshio southeast of Taiwan and its possible forcing mechanism

Yi-Chia Hsin · Tangdong Qu · Chau-Ron Wu

Abstract The intra-seasonal variation of the Kuroshio southeast of Taiwan has been studied using satellite data and a numerical model. Superimposed with the main stream of the Kuroshio, two intra-seasonal signals are revealed in the study region. The fluctuation with a period of 1–6 months results from offshore eddies. The westward propagating cyclonic eddies can reduce or reverse the northward flow east of the Kuroshio between 121° and 123° E, but only slightly touch the core velocity of the Kuroshio. The fluctuation with a period of 2–4 weeks is only significant between Taiwan and the Lan-Yu Island (the low-velocity region). Different mechanisms are responsible for the fluctuation in the low-velocity region in different seasons. In winter, the change of negative wind stress curl in the northeastern South China Sea modulates the circulation southeast of Taiwan, while the typhoon-induced intense wind is responsible for the current fluctuation in summer.

Keywords Intra-seasonal variation ·
Kuroshio southeast of Taiwan

Y.-C. Hsin · C.-R. Wu (✉)
Department of Earth Sciences,
National Taiwan Normal University,
88, Section 4 Ting-Chou Road,
Taipei 11677, Taiwan
e-mail: cwu@ntnu.edu.tw

Y.-C. Hsin · T. Qu
International Pacific Research Center, School of Ocean and Earth
Science and Technology, University of Hawaii,
Honolulu, HI, USA

1 Introduction

The Kuroshio closes the subtropical gyre on the western boundary of the North Pacific basin. When the North Equatorial Current arrives at the east coast of the Philippines, it bifurcates into two branches. The northern branch is the Kuroshio (e.g., Qu and Lukas 2003). After branching, the Kuroshio continues flowing northward along the east coasts of Luzon and Taiwan, the shelf slope of the East China Sea, and the south coast of Japan, and eventually becomes the Kuroshio Extension off Japan. The flow pattern becomes complicated when the northward-flowing Kuroshio reaches the Luzon Strait, a western land boundary gap. There, the Kuroshio either loops into the South China Sea or bypasses the Luzon Strait in a straight path (e.g., Wu and Chiang 2007; Hsin et al. 2008). Different pathways of the Kuroshio in the Luzon Strait may have distinct effects on the behavior of the downstream Kuroshio, especially the regions southeast of Taiwan. As a result, the Kuroshio southeast of Taiwan is highly variable both in time and space.

Based on in situ hydrographic surveys east of Taiwan, temporal and spatial variations of the Kuroshio have been observed from cruise to cruise (Chu 1974). Its transport varies in a large range of timescales from days to years (e.g., Johns et al. 2001; Gilson and Roemmich 2002; Hwang and Kao 2002; Hsin et al. 2008). In addition to the seasonal variation, the most pronounced signal in the region due to the reversal of East Asian Monsoon, the intra-seasonal variations are also observed. There are several factors contributing to these variations. Among others, the strong influence of intra-seasonal atmospheric forcing has been identified. As a special case of this atmospheric forcing, an intra-seasonal oscillation with a quasi-periodicity of 30–60 days is well-known in the tropical atmosphere as

the Madden-Julian-Oscillation. This intra-seasonal signal could be injected into the ocean as a result of local and/or remote air–sea interaction.

Besides the atmospheric forcing, eddy activity, bottom topography, and baroclinic instability are also thought as possible causes inducing intra-seasonal variations in the ocean (e.g., Zhang et al. 2001; Kessler 2005). The intra-seasonal variations with timescales from days to months in the region around Taiwan have been documented in the literature. Wu et al. (2008), by means of numerical simulations, related the appearance of cold dome off northeast Taiwan to the intra-seasonal migration of the Kuroshio with two dominant periods centered at ~30 and ~70 days. Based on a mooring array deployed along the PCM-1 line (at ~24.5° N) during the World Ocean Circulation Experiment, Zhang et al. (2001) suggested that the velocity variability on the period band between 30 and 70 days is generated by the Kuroshio self-instability. The band-passed root-mean-square of the TOPEX/Poseidon-based sea surface height also demonstrated that the region east of Taiwan is highly variable on the intra-seasonal timescales of 35–85 days (Kessler 2005). Off southwest Taiwan, Wu et al. (2005) attributed the intra-seasonal variation of local wind stress curl (WSC) to the alternation of flow direction observed by a pair of moorings with up-looking Acoustic Doppler Current Profilers (ADCPs) ["W" and "E" in Fig. 1]. From the conjunction of drifters,

TOPEX/Poseidon satellite altimeter, and Advanced Very High Resolution Radiometer (AVHRR) sea surface temperature data, Jing and Li (2003) noted that an event-like cold-core, cyclonic Kuroshio frontal eddy existed between southern Taiwan and the Lan-Yu Island and persisted for about 2 months around March 1996. This cold-core eddy accompanied an offshore meander of the Kuroshio near the Lan-Yu Island.

Moreover, the intra-seasonal variations on longer time-scales of 100~200 days off eastern Taiwan are often introduced as a result of interaction between the Kuroshio and offshore eddies originating in the interior Pacific. Hsin et al. (2008) suggested that the impingement of mesoscale eddies can alter the velocity and path of the Kuroshio, which in turn can alter the water input into the East China Sea, and is believed to be an important driver of the intra-seasonal variations in the region. Zhang et al. (2001) suggested that these mesoscale eddies have periods between 70 and 200 days. In addition to the direct interaction between the Kuroshio and eddies from the east along the latitude band of 22–25° N, eddies can also be brought by the north-flowing Kuroshio from the further upstream region around the Luzon Island and Strait (Sheu et al. 2010). As Ichikawa (2001) and Ichikawa et al. (2008) have suggested, the mesoscale eddies impinging the Kuroshio south of the East Taiwan Channel ("ETC" in Fig. 1) can also influence the flow field in the southern East China Sea and pass their variability through the Kuroshio to the volume transport at the Takara Strait in the northeastern East China Sea.

This study focuses on the intra-seasonal variation southeast of Taiwan, especially in the low-velocity region ("L" in Fig. 1) between Taiwan and the Lan-Yu Island. By the use of satellite data (altimetry and sea surface wind) combined with simulation from a well-validated numerical ocean model, we attempt to investigate the intra-seasonal variation of the Kuroshio in the upper ocean southeast of Taiwan. In Section 2, the data used in this study are introduced. Section 3 presents and discusses the results of the analyses. Some possible mechanisms related to the Kuroshio intra-seasonal variations are also discussed in this section. The conclusions are given in the final section.
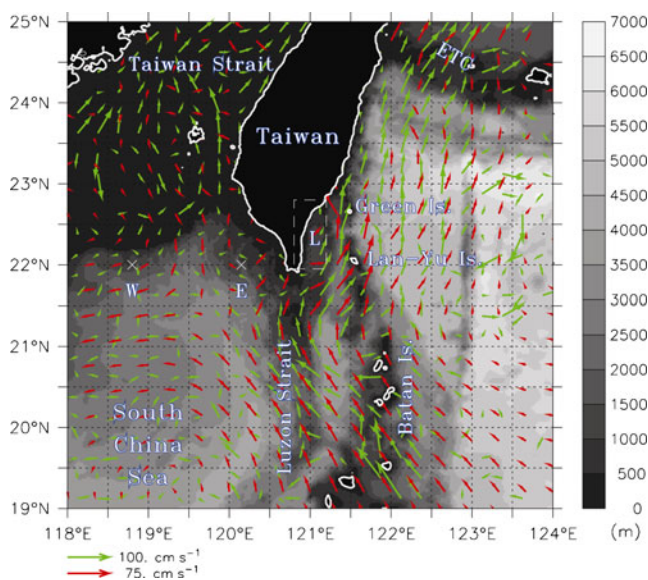

Fig. 1 Bathymetry and mean surface flow around Taiwan. The *green arrows* denote the annual mean flow average from 20 to 300 m compiled with the Sb-ADCP data from 1991 to 2005 by the National Center for Ocean Research, Taiwan, http://www.ncor.ntu.edu.tw. The *red arrows* are the mean geostrophic current (1993–2007) which is derived from the altimeter-based sea level anomaly by AVISO. W and E are the locations of moorings used in Wu et al. (2005). The *dashed frame* marked with "L" represents the low-velocity region. *ETC* indicates East Taiwan Channel

2 Satellite data and model description

The gridded multi-satellite altimeter-based mean sea level anomaly (SLA) and mean geostrophic velocity are used in this study. The products were distributed by Archiving, Validation and Interpretation of Satellite Oceanographic (AVISO) data and obtained from http://www.aviso.oceanobs.com/. They were merged from five altimeter missions: ENVISAT, ERS-1 and ERS-2, GFO, Jason-1, and TOPEX/

Poseidon, and have resolutions of 1/3° in space and 7 days in time. The gridded altimeter-based products are available from October 1992 to the present. The wind stress data used in this study were derived from a time and space blend of the QuikSCAT-DIRTH satellite scatterometer observations and the National Center for Environmental Prediction (NCEP) analyses (QSCAT/NCEP; Milliff et al. 1999) and have a horizontal resolution of a half degree with a time interval of 6 h for the period after July 1999. The data were distributed by the Data Support Section of the National Center for Atmospheric Research (http://dss.ucar.edu/). Combined with the NCEP reanalysis version 2 wind product with a horizontal resolution of 2.5°, we extended the time of wind data back to 1993. Firstly, the NCEP reanalysis wind product is linear-interpolated onto the grid of QSCAT/NCEP wind.

Altimeter-based geostrophic velocity is used to investigate the temporal and spatial variation of the Kuroshio in the upper ocean of the area studied. Figure 1 shows the annual mean surface flow from the shipboard-ADCP (Sb-ADCP) observations (green arrows) and the geostrophic velocity (red arrows) derived from the satellite altimetry SLA. The mean flow pattern of the altimeter-based velocity is quite similar to that of Sb-ADCP-based velocity, which was composited with observations between 1991 and 2005, except for some quantitative differences in magnitude. This is particularly true in the regions around the Luzon Strait and eastern Taiwan, including the intrusion position and pathway of the Kuroshio. A low-velocity region on the shore side of the Kuroshio (shown in the drifter map of Centurioni et al. (2004); indicated by letter "L" in Fig. 1) is also well reproduced by this satellite product. Since the altimeter-based geostrophic velocity resolves temporal and spatial scales of interest, we use the data to discuss the variability of the surface Kuroshio off southeast Taiwan.

In addition, the East Asian Marginal Seas (EAMS) model based on the Princeton Ocean Model (POM; Mellor 2004) is also used in this study. This model has been used to investigate the variations of volume transport and flow field in different depth ranges in the seas east and west of Taiwan (Wu and Hsin 2005; Hsin et al. 2008). Hsin et al. (2008) also used this model to study the impact of the westward-propagating eddies on the flow east of Taiwan on the timescale of about 100 days. The EAMS model covers a domain of 99–140° E and 0–42° N with a resolution of 1/8° in horizontal and has 26 sigma levels in vertical. The model is forced by the 6-hourly half-degree resolution blended QSCAT/NCEP wind product, which is gained after July 1999, and the weekly 1° AVHRR sea surface temperature. A North Pacific Ocean Model, which has an extended domain of 99° E–77° W and 16° S–60° N with a horizontal resolution of 1/4°×1/4° and the same vertical sigma levels as the EAMS model, serves the open boundary conditions of the EAMS model at a 1-day time interval using one-way

nesting method. Careful validations for the EAMS model have been made in Wu and Hsin (2005) and Hsin et al. (2008), respectively, for the regions west and east of Taiwan. The simulation period spans from 2000 to 2005. The detailed information about this model is referred to Hsin et al. (2008), and the basic hydrodynamic content of POM is consulted in Mellor (2004).

3 Results

3.1 Mean current structure off southeastern Taiwan

As shown in Fig. 1, when the Kuroshio arrives in the vicinity of the Luzon Strait, a branch of it intrudes westward into the northern South China Sea from the middle of the Luzon Strait around 20.75° N and 120.75° E. Most of the Kuroshio water circulates in a saddle-shape and returns to the east at the southern tip of Taiwan. The main stream of the Kuroshio flows straightly along the west side of the Batan Islands to the east coast of Taiwan. After leaving the Luzon Strait, the core of the surface Kuroshio always passes around the Lan-Yu Island at 121.5° E, 22° N to the north and reaches its maximum speed around 24° N. Between the Kuroshio and southeastern coast of Taiwan, a low-velocity region is visible in both surface flow products. Some speedy flow passes east of the Lan-Yu Island and forms the Kuroshio "offshore path" as proposed by Hsin et al. (2008). The mean offshore path extends to 123° E at 22° N (Hsin et al. 2008).

3.2 Variability of geostrophic velocity off southeastern Taiwan

To show the temporal variation of the meridional component of geostrophic velocity (GSV) southeast of Taiwan, the GSV along 22° N from January 1993 to December 2007 is depicted in Fig. 2. The high GSV (red-color shading) takes place mostly between 121° and 123° E near the Lan-Yu Island (121.5° E, bold black dash line and noted as "LY" in Fig. 2). Again, this result indicates that the Kuroshio main stream always passes around the Lan-Yu Island, despite some west–eastward swings with time. The main stream of the Kuroshio gets closer to the coast of Taiwan and tends to have a stronger GSV in summer than in winter, which coincides with the seasonal change of the surface flow observed from the high-frequency ocean radar off northeast Taiwan (Ichikawa et al. 2008). In some occasions (e.g., spring 1996 and summer 2004), the main stream (see the red shading in Fig. 2) of the Kuroshio has been observed as far as 123° E in the surface layer.

The GSV near the east coast of Taiwan (~121° E, black line in Fig. 3), i.e., between Taiwan and the Lan-Yu Island,
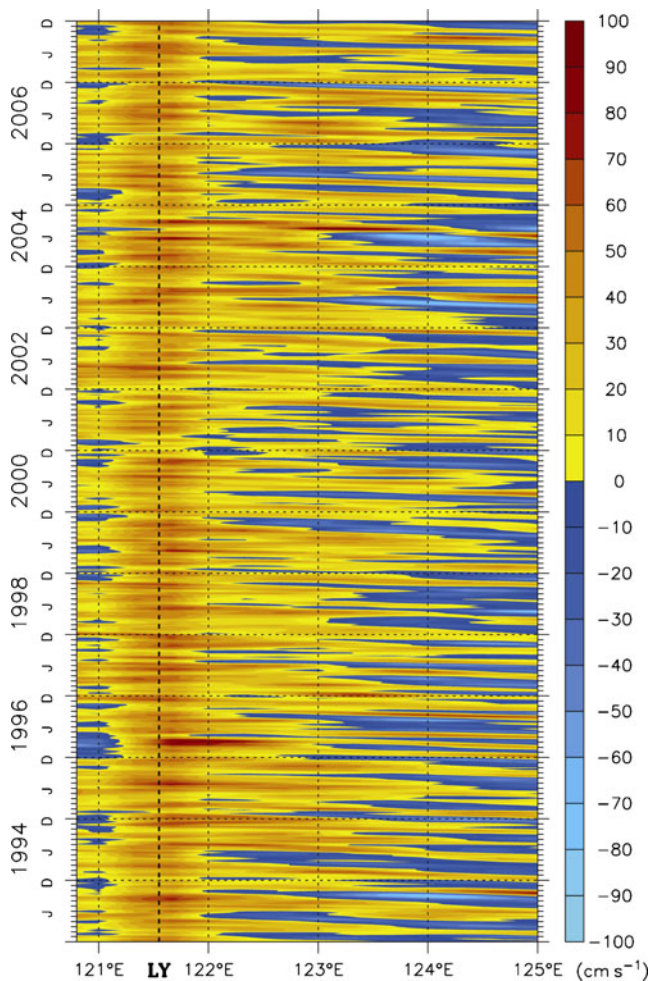
Fig. 2 Meridional geostrophic velocities (GSV) off southeast Taiwan between 120.75° and 125° E. The GSV is depicted along the latitude of 22° N. LY denotes the Lan-Yu Island and is depicted by the *bold black dash line*. The *positive sign* (*warm color*) represents the northward GSV. The *cold color* is used for the southward GSV (negative velocity)
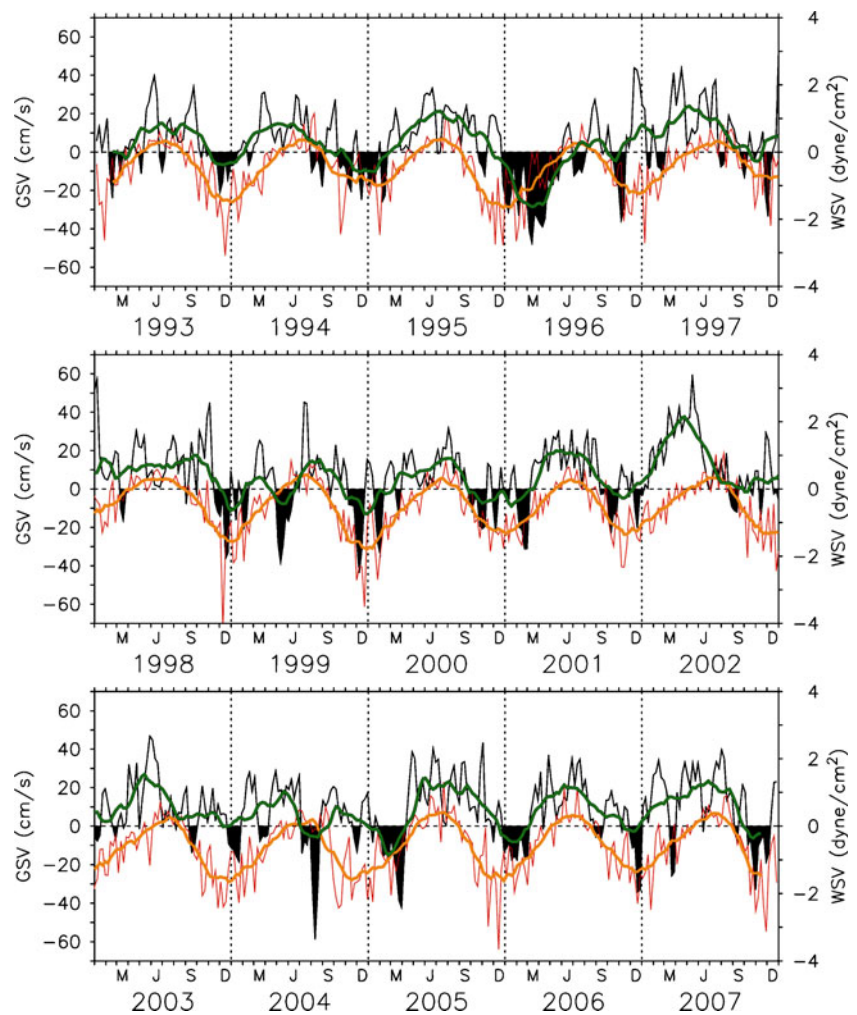
can turn from a northward flow (the maximum northward velocity is about 60 cm s^{-1}) to a southward flow (curve with black shading, the maximum southward velocity reaches about −60 cm s^{-1}) in an irregular time interval. Counting from the GSV at 121° E, 22° N, there are 68 southward-flow events in the 15-year period between 1993 and 2007. The duration of southward-flow events ranges from 7 to 160 days with an average of 26 days. The southward-flow events take place most frequently during winter (here, summer is defined as May–September, and winter is defined as the remaining 6 months) and can persist over 1 month with an average of 28 days. In summer, the southward-flow events persist at a shorter time span centered at 18 days. The most significant summertime southward-flow events occurred in August–September 1994, July–August 1996, May–June 1999, and July–August 2004, all of which had durations of 1–2 months.

The GSV at 121° E, 22° N and local meridional wind stress (120–123° E, 21–24° N) around eastern Taiwan are generally in good correlation on the seasonal timescale (shown as the green and orange bold lines in Fig. 3), despite some quantitative discrepancies in some years (e.g., 1996 and 2004). In summer (winter) when the wind prevails in the northward (southward) direction, the GSV tends to have northward (southward) velocities (Fig. 3). However, they do not show a good correlation in the higher frequency time series (black and red lines), in which the intra-seasonal variation is expected to play a more significant role.

The southward-flow events also take place farther seaward of the Lan-Yu Island between 122° and 123° E (Fig. 2), roughly coinciding with the mean eastern bound of the Kuroshio at this latitude (Liang et al. 2003; Hsin et al. 2008). However, the southward-flow incident at 122.75° E, 22° N seems to have a longer lapse (49 events in 15 years) and a shorter duration between 7 and 80 days, with an average of 22 days, in comparison with that of 26 days near the Taiwan coast. The occurrence of the southward-flow events east of the Lan-Yu Island does not have a distinct seasonal variation and the southward-velocity signals seem to originate from the eastern boundary (Fig. 2), inferring the impact from the east. Satellite observations have shown the abundance of eddies in the Pacific subtropical regions, especially north of 10° N (Hwang et al. 2004). These westward-propagating eddies reach the study area where they interact with the Kuroshio and modulate the Kuroshio's transport and path. The impact of eddies on the Kuroshio east of Taiwan has been reported in the literature (e.g., Yang et al. 1999; Johns et al. 2001; Zhang et al. 2001; Hwang and Kao 2002; Hsin et al. 2008; Ichikawa et al. 2008).

Furthermore, the preserving variance spectrum based upon the fast Fourier transform method is conducted to identify the dominant frequency of the GSV variations on both sides of the Kuroshio around the Lan-Yu Island (Fig. 4). On the west side of the Kuroshio (between the southern tip of Taiwan and the Lan-Yu Island, Fig. 4a), two significant peaks are revealed on the period band of 2–4 weeks (14–28 days). These two peaks do not appear on the east side of the Lan-Yu Island (Fig. 4b). On the period bands of ~60 and ~180 days, two energetic peaks are seen on both sides. However, the peaks on 77, 128, and 168 days are only visible east of the Lan-Yu Island. For the period longer than half a year, the annual signal (~365 days) associated with the seasonally reversing monsoon is present on the west side of the Lan-Yu Island. The seasonal signal on the east side of the Lan-Yu Island may be hidden due to the strong impact of the mesoscale eddies from the east. From the 20 months of observations along the PCM-1 (~24.5° N), Johns et al. (2001) also noticed no seasonal

Fig. 3 Time series of GSV in the low-velocity region and WSV near southeastern Taiwan. The GSV is the meridional geostrophic velocity at 121° E and 22° N. The negative (southward) GSV is filled with *black color*. The WSV is averaged over 120–123° E and 21–24° N. The *red line* denotes the WSV with 7 days′ running average. The *bold lines* are 91 days′ running averaged time series of GSV (*green*) and WSV (*orange*)
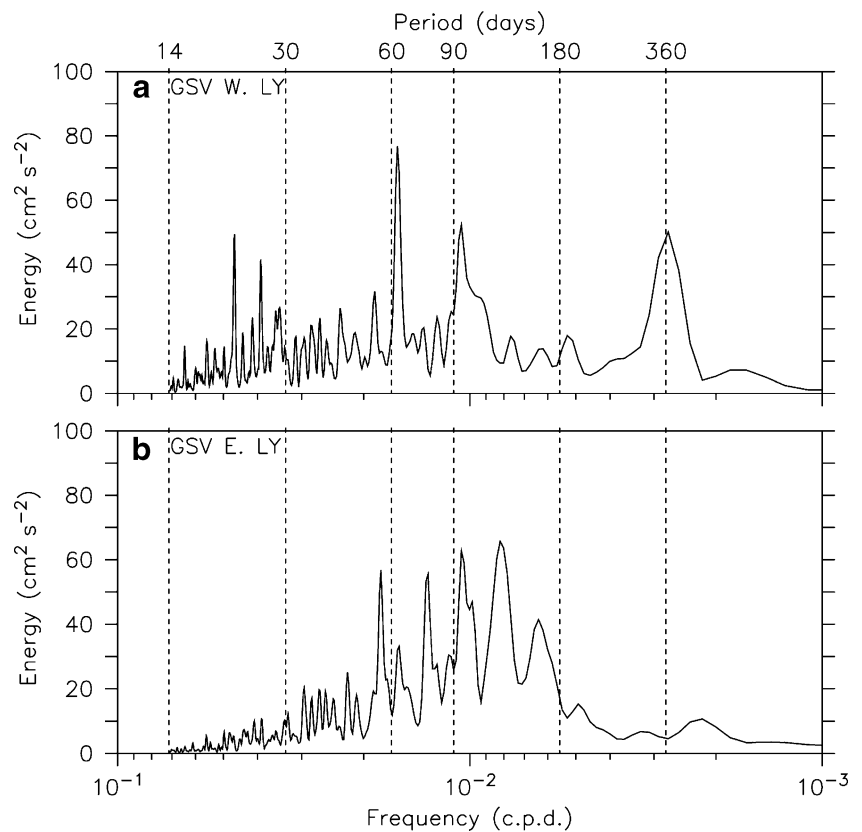

trend in the transport time series. In summary, three groups of signals (2–4 weeks, 1–6 months, and 1 year) can be found on the west side of the Kuroshio, but only one group (1–6 months) is obvious on the east side.

Figure 5 shows time series of the GSV southeast of Taiwan (red curves) and the zonal geostrophic velocity (GSU) southwest of Taiwan (blue curves). For clarity, a 13-points (91 days) Hanning window smoother is applied to the data (the bold lines in Fig. 5). At times, the variation of the GSV on the east side of Taiwan (121–121.33° E, 22° N) has a good correspondence with that of the GSU off the west coast of Taiwan (120.33° E, 21.77° N). In some particular cases, a strong eastward (positive) GSU southwest of Taiwan accompanies a weak or southward (negative) GSV near the southeast coast of Taiwan. Nevertheless, this does not seem to be always true for the period of observations, since the correlation coefficient between the two time series is only about 0.18. Of interest is that the correlation can be reached as high as ~0.6 while only wintertime data are applied, implying that the GSV between Taiwan and the Lan-Yu Island in winter can be

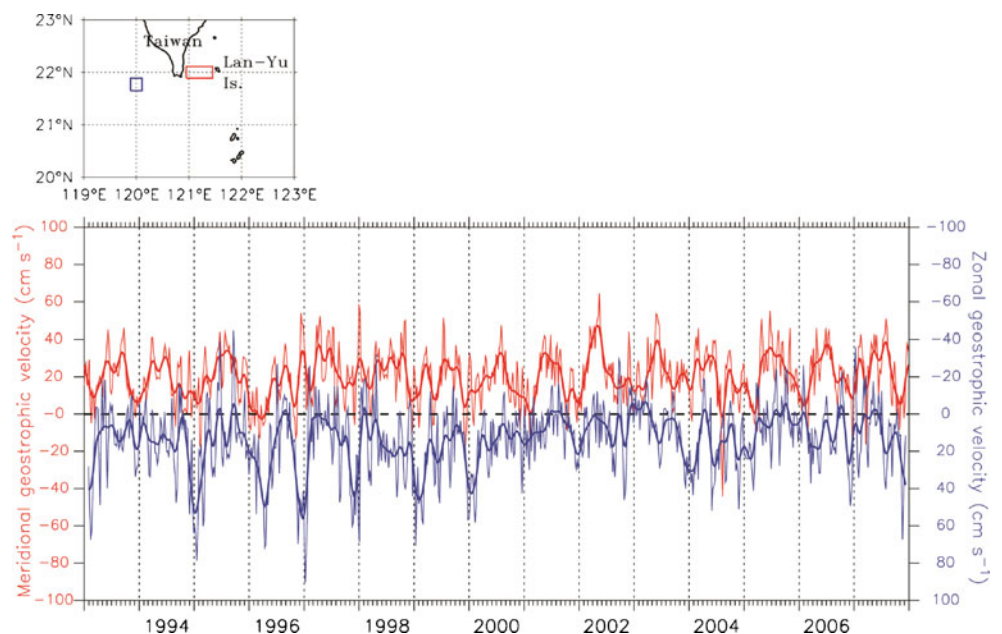greatly affected by (or highly related to) the variation of the GSU off southwestern Taiwan.

In addition to the intra-seasonal variations discussed above, clear seasonality is also observed in the GSV southeast of Taiwan and the GSU southwest of Taiwan (Fig. 5). The seasonal variation of the GSU southwest of Taiwan seems to have a good agreement with the seasonal Kuroshio intrusion in the Luzon Strait. The Kuroshio in the Luzon Strait often forms a loop current in winter and tends to have a straight path in summer (Wu and Chiang 2007). As a consequence, the eastward GSU southwest of Taiwan in winter can be regarded as part of the looping Kuroshio. When the Kuroshio in the Luzon Strait follows a straight path in summer, the GSU southwest of Taiwan slows down or turns westward (negative velocity). The seasonal variability is also demonstrated in the composite plots of summer and winter (Fig. 6a, d). The seasonal reversal of monsoonal wind, which not only shows an opposite wind direction but also makes a highly different spatial distribution of WSC, can contribute to the flow's seasonal variation of the region. As shown in Fig. 6a, d, the wind stress field

displays a strong seasonality, with weaker (<0.05 N m^{-2}) and southwesterly wind in summer and stronger (>0.15 N m^{-2}) and northeasterly wind in winter. Similar to the wind stress, the WSC off southwest Taiwan also varies from season to season. Due to the impeded land mass, the monsoonal wind induces a strong negative WSC off southwest Taiwan in winter but not in summer.
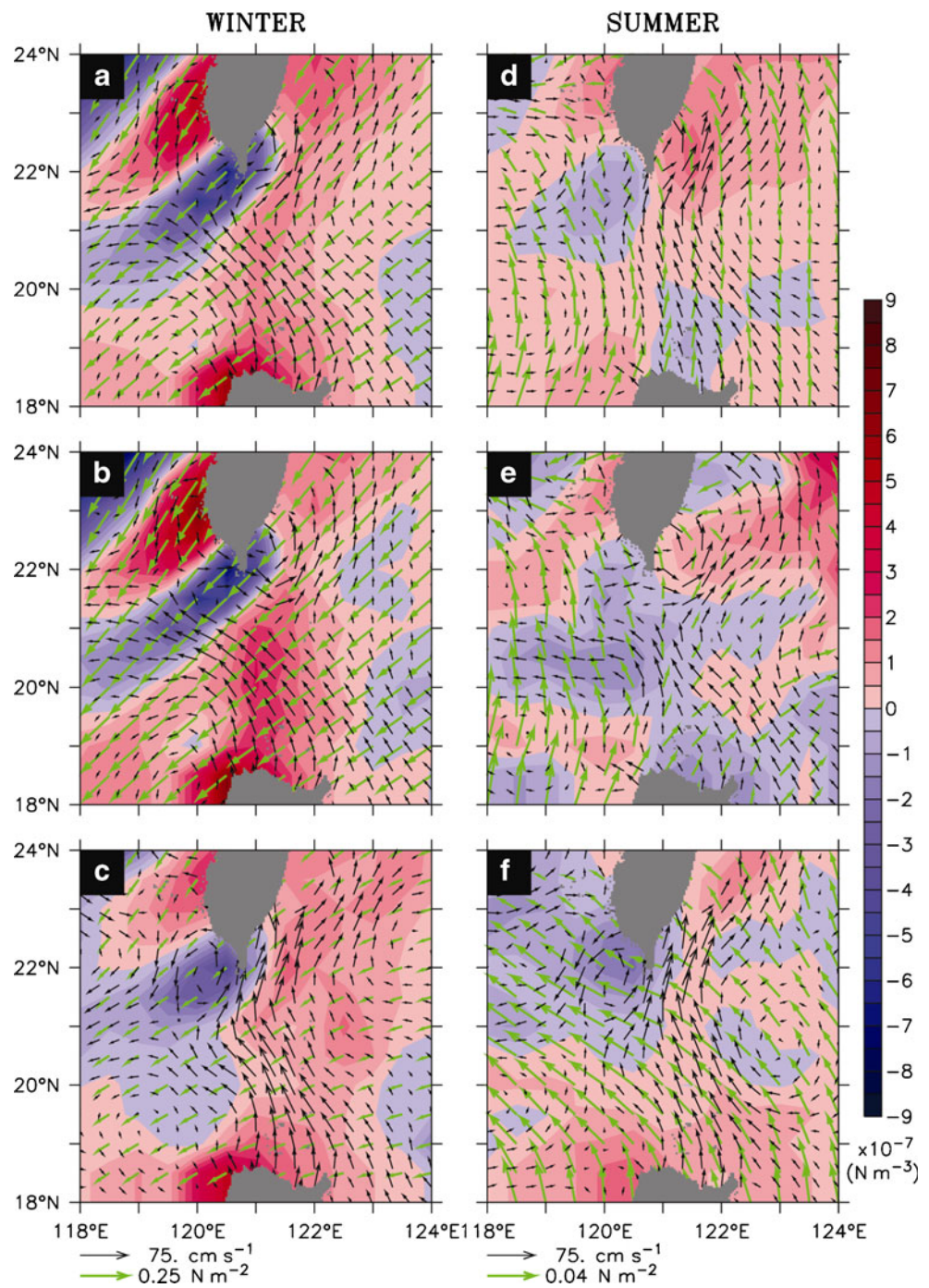
3.3 Forcing mechanism for the Kuroshio intra-seasonal fluctuations in winter

As mentioned above, the lapse of the meridional velocity reversal between Taiwan and the Lan-Yu Island is shorter than that east of the Lan-Yu Island. Looking over the entire observational period from 1993 to 2007 (Fig. 2), much

Fig. 5 Time series of the geostrophic components off southeast and southwest Taiwan. The *red lines* are the GSV off southeast Taiwan (*red frame in the upper panel*), and the *blue ones* represent the GSU off southwest Taiwan (*blue frame in the upper panel*). The *thin lines* are the original time series with a time interval of 7 days. The *thick ones* denote the smooth time series with a 13-points' (91-days') Hanning smoother. The zero velocity line is depicted as the *bold black dash line*. For GSU (*blue lines*), the axis is reversed from −100 cm s^{-1} at top to 100 cm s^{-1} at bottom. The positive GSV and GSU are toward the north and east, respectively

Fig. 6 Geostrophic current, wind stress, and wind stress curl (**a**) averaged over winters of 1993–2007, **b** a composite of the southward-velocity events in winter during the period of 1993–2007 as indicated in Fig. 3, **c** a composite of the northward-velocity events in winter, **d** same as **a** but for summer, **e** same as **b** but for summer, and **f** same as **c** but for summer. The *black arrows*, the *green arrows*, and the *color shading* represent the geostrophic current, the wind stress, and the wind stress curl, respectively. The unit lengths of wind stress are 0.04 and 0.25 N m^{-2} for summer and winter, respectively

more southward-flow incidents between Taiwan and the Lan-Yu Island have been observed during winter. One possible process responsible for these incidents is related to the variation of the GSU southwest of Taiwan (Fig. 5). In contrast, the events east of the Lan-Yu Island may heavily depend on the impingement of the westward propagating cyclonic eddies from the interior ocean. In use of data from in situ field works, mooring array, satellite altimeter, and numerical modeling, Yang et al. (1999), Yang and Liu

(2003), Johns et al. (2001), and Hsin et al. (2008) have discussed the Kuroshio–eddy interaction processes around eastern Taiwan, as described in the Section 1.

Because the East Asian Monsoon is the major atmospheric forcing in the study region, the GSV and the meridional wind stress are highly correlated on the seasonal timescale. On the intra-seasonal timescale, on the other hand, their correlation is relatively weak (above-mentioned in Section 3.2). To further look into the relationship

between the wind field and geostrophic current field, the composite plots are made. For the period between 1993 and 2007, composites of northward- and southward-velocity events based on the altimeter-based meridional geostrophic velocity are depicted in Fig. 6b, c, e, and f. The critical values of velocity selected for the composites are −10 cm s^{-1} (mean − 1 standard deviation) for the southward-velocity events and 24 cm s^{-1} (mean+1 standard deviation) for the northward-velocity events.

Revealed from Fig. 6, the wind patterns are out of phase between seasons, southwesterly wind in summer and northeasterly wind in winter. However, regardless of seasons, the composite geostrophic current maps show a similar pattern around southern Taiwan. When the surface current off southeast Taiwan flows to the south (the southward-event composite), a clockwise loop (anti-cyclone) appears off southwest Taiwan, and the Kuroshio with a larger intrusive angle is present in the middle of the Luzon Strait (Fig. 6b, e). On the other hand, when the surface current off southeast Taiwan flows to the north (the northward-event composite), the surface current flows in a straight path in the Luzon Strait and forms a cyclonic circulation off southwest Taiwan (Fig. 6c, f). The fact indicates that the negative WSC off southwest Taiwan in winter is favorable for the development of Kuroshio loop current in the Luzon Strait (Fig. 6b, c), as well as for the generation of the Kuroshio offshore path southeast of Taiwan.

Furthermore, the magnitudes of WSC in winter (Fig. 6a–c) are always much larger than those in summer (Fig. 6d–f), implying that the magnitude of WSC is not the key factor influencing the flow off southern Taiwan. The change of magnitude of WSC is critical in altering the GSU off southwestern Taiwan and further influence the GSV off southern Taiwan in winter. On the other hand, the composites of WSC in summer (Fig. 6e, f) are not similar to those in winter, when the southward-event composite WSC off southwest Taiwan (Fig. 6b) is larger than the northward-event composite one (Fig. 6c). Therefore, in summer, different processes seem to work on causing the current to flow southward in the low-velocity region (Fig. 6e, f), which is discussed in Section 3.4.

The good correspondence between the change of WSC off southwest Taiwan and the flow off southeast Taiwan can be further explained as follows. Using a mooring pair off southwest Taiwan during October 2000–April 2001, Wu et al. (2005) speculated that the enhanced negative WSC off southwest Taiwan would generate an anti-cyclonic circulation that in turn would help the development of a loop current in the Luzon Strait. Our analysis lends support for the earlier speculation of Wu et al. During the periods from November 23 to December 14, 2000 and from February 28 to March 07, 2001, when the
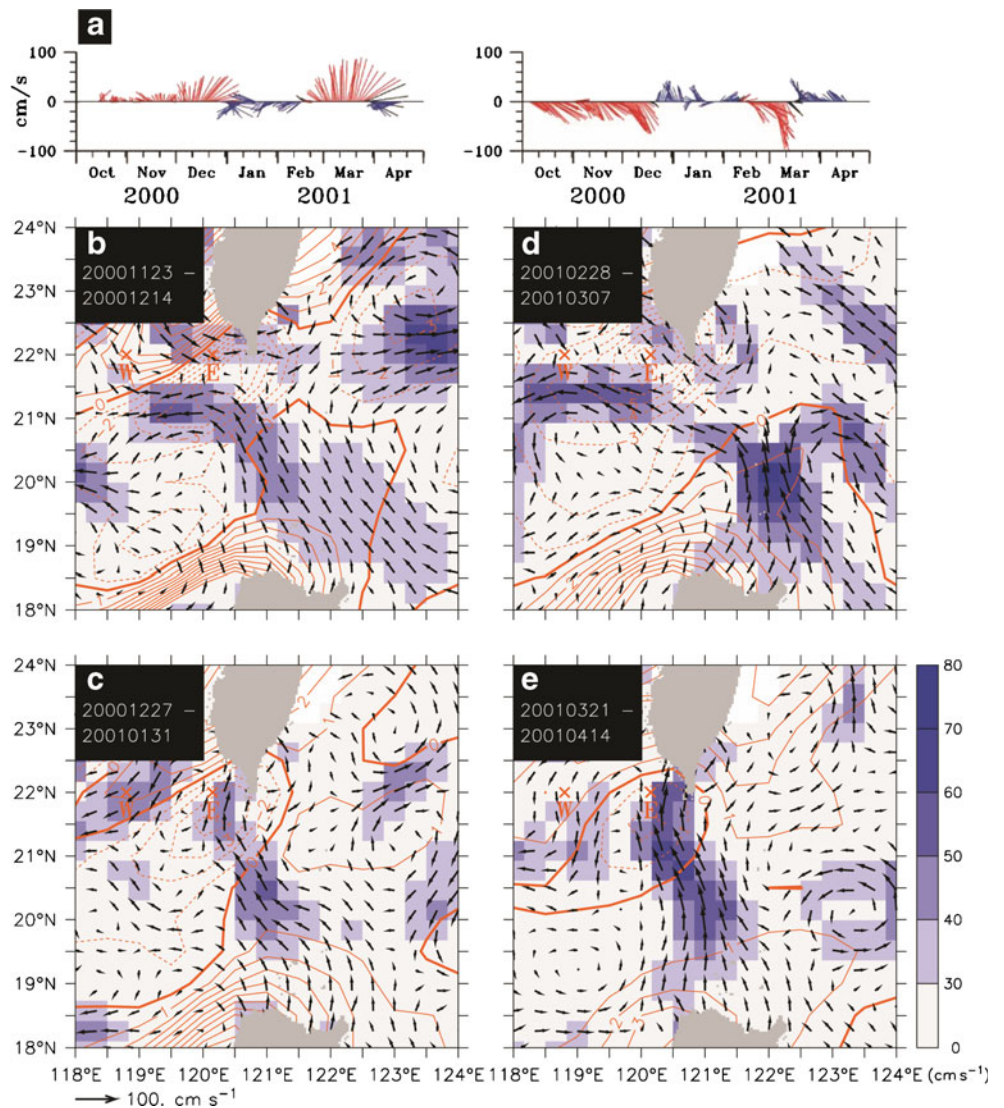
mooring velocity is southeastward at station E and northward at station W (Fig. 7a), a looping branch of the Kuroshio is markedly evident in the Luzon Strait (Fig. 7b, d). The Kuroshio loops westward into the South China Sea and apparently contributes to a clockwise circulation around the two mooring stations. The southeastward flow at station E, which can probably be regarded as the northern flank of the anti-cyclonic loop current, further triggers an eastward shift of the main axis of the Kuroshio near the sea surface. As a consequence, the velocity between Taiwan and the Lan-Yu Island slows down. On the contrary, a weakened WSC west of the Luzon Strait may result in a straight path of the Kuroshio that strengthens the velocity between Taiwan and the Lan-Yu Island (Fig. 7c, e).

3.4 Forcing mechanism for the Kuroshio intra-seasonal fluctuations in summer

Unlike the situation in winter, the correlation between velocity components southeast and southwest of Taiwan is fairly poor in summer. This indicates that the WSC off southwest Taiwan and the intrusion of the Kuroshio in the Luzon Strait cannot explain the variation of the GSV between Taiwan and the Lan-Yu Island in this season. Due to the speedy translation of typhoons in a short period (hours to days), it is hard to find close relations between the typhoon-induced wind and geostrophic current in the composite fields (Fig. 6e). Of interest is a northerly wind component to the north of the low-velocity region. Between 1993 and 2007, there were 14 summertime southward-velocity events selected to compose Fig. 6e. Among them, 12 events were formed when the tropical cyclones or typhoons passed around Taiwan and induced northerly wind east of Taiwan. That is to say, that ~85% (12/14) of summertime southward-velocity events can be attributed to the influence of typhoons, suggesting that the formation of southward-velocity events is highly related to the local typhoon-induced wind around the eastern Taiwan.

Accordingly, we hypothesize that the frequent visiting of tropical cyclones (typhoons) is a mechanism responsible for the summertime current variation. Typhoons coming from the western Pacific Ocean or South China Sea usually visit Taiwan in April–November every year, with a peak period in July–September. Figure 8 shows the wind and SST distributions east of Taiwan and impingement of typhoons on the region in summer (May–September). High-frequency fluctuation is revealed in wind field. In few days after a typhoon's visit, the wind stress can suddenly become very large either to the north or south, depending on the typhoon's path, which in turn will lead to a big drop in SST (Fig. 8). In average, there are 6.7 typhoons passing through

Fig. 7 **a** Stick plots of mooring pair off southwest Taiwan during October 2000–April 2001, after Fig. 5 of Wu et al. (2005). The *blue* and *red sticks* in panel **a** denote different episodes. Averaged altimeter-based geostrophic current and its corresponding wind stress curl (contour lines) are in **b** November 23, 2000–December 14, 2000, **c** December 27, 2000–January 31, 2001, **d** February 28, 2001–March 07, 2001, and **e** March 21, 2001–April 14, 2001. *Arrows* in **b**–**e** represent geostrophic current, and color shading is the quantity of geostrophic current. Stations W and E are also depicted in **b**–**e**. The contour interval for the wind stress curl is 1×10^{-7} N m^{-3}

the vicinity of Taiwan between May and September each year. Although the GSV in the low-velocity area (Fig. 3) does not always reverse to a southward velocity, the impingement of typhoons can still exert an immediate impact on the surface flow around Taiwan. It can also cool down the water temperature in the ocean's surface layer through Ekman pumping and vertical entrainment. When a typhoon sweeps the ocean surface, it injects a large amount of kinetic energy into the ocean surface layer, and then generates vertical and horizontal motions of sea water. As shown in Fig. 3, the two most obvious southward-velocity events were in March–June, 1999, and July–August, 2004, and both periods were related to the visiting of typhoons.

A series of numerical experiments are performed to further investigate the relationship between variations in local typhoon-induced wind and surface flow. In summer, the short-term fluctuations of wind speed around Taiwan take place rather frequently. During these high-frequency fluctuations, the wind can reverse its direction within a short time period. These changes in wind can immediately affect the surface flow and temperature southeast of Taiwan. A single event of wind reversal can sometimes make the northward surface current in the low-velocity region slow down (when the original flow velocity is high) or even turn southward (when the original flow velocity is low) in a few days. Another immediate consequence of these wind fluctuations is a temperature drop near the sea surface. A sequential of wind reversal events would persistently weaken the surface flow and sustain a cold surface temperature in the low-velocity region for 1–2 months.

Three examples are taken here to discuss the summer-time current variations associated with the typhoon-induced wind changes (Figs. 9, 10, and 11). The first example was the super typhoon Mindulle in late June 2004, a slow-down in surface current and a temperature drop took place just
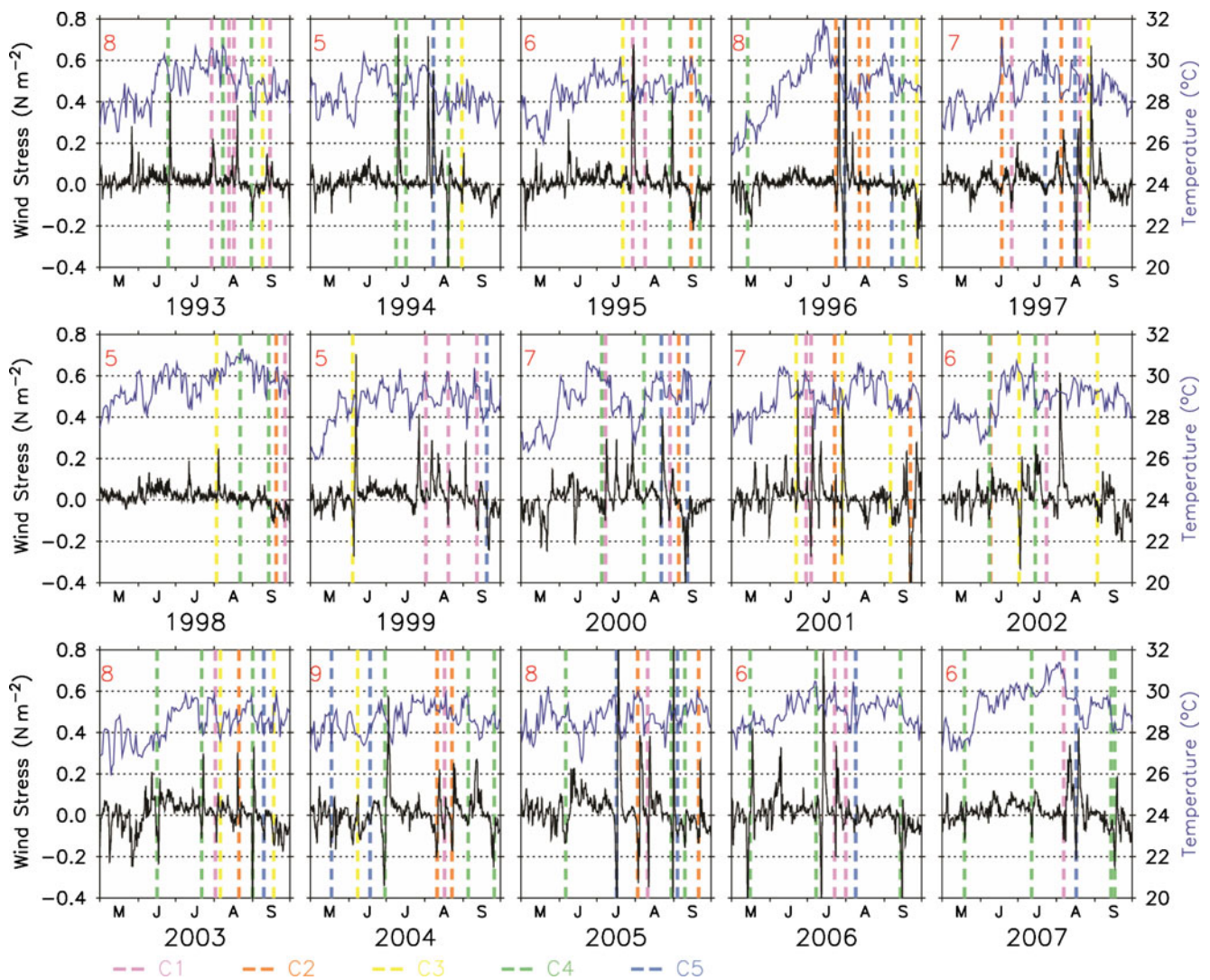
Fig. 8 WSV and SST in summers (May–September) between 1993 and 2007. The WSV (*black*) is averaged over 120–123° E and 21–24° N. The AVHRR-based SST (*blue*) is located at 120.75° E, 22° N. The *dashed lines* denote the eve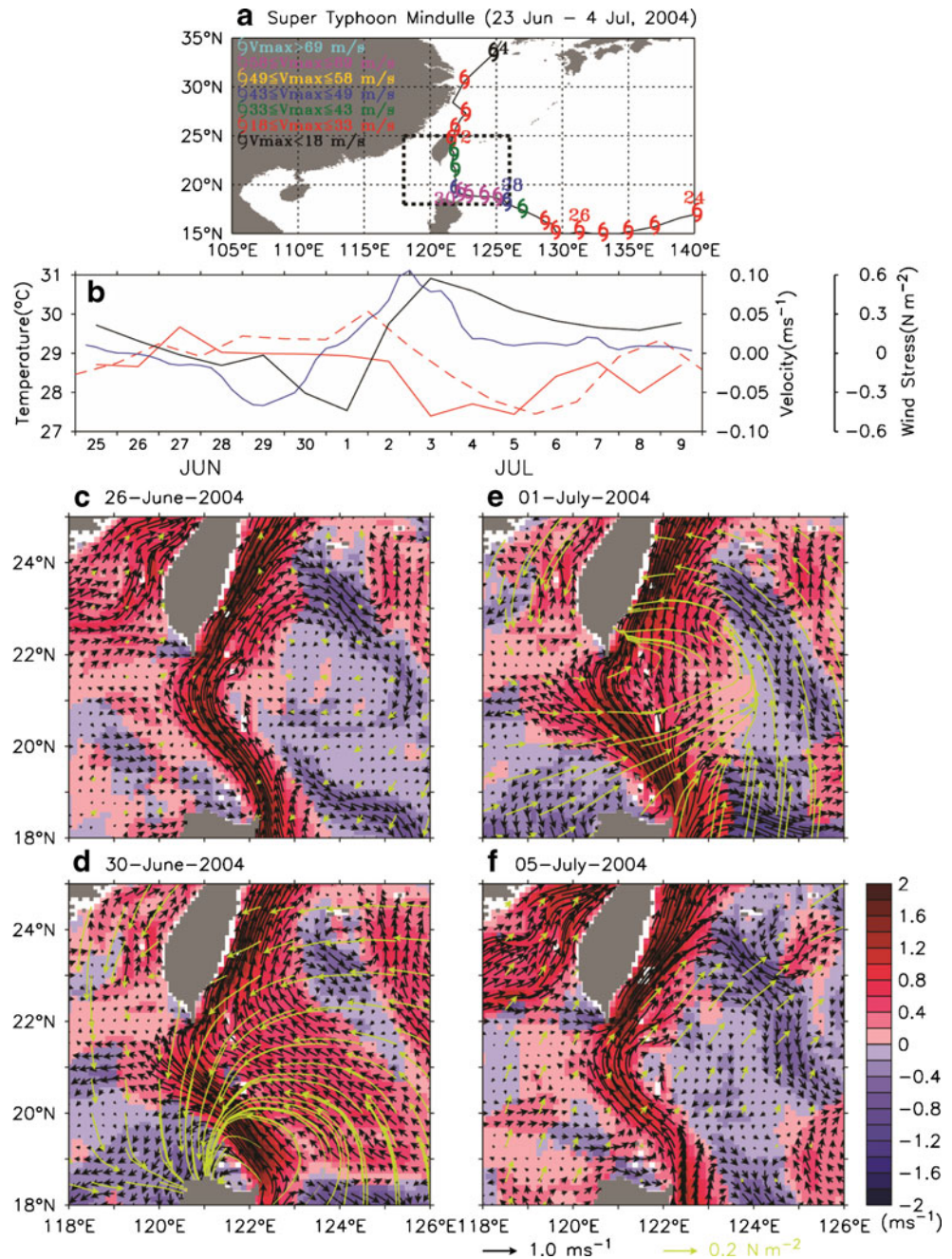nts of typhoon impinging in the neighbor-hood of Taiwan, and the different colors represent different strengths of typhoon on Saffir–Simpson scale (category 1 to 5, C1~C5). Number of typhoon events each year is marked at the *upper left corner*

after a sudden wind change when Mindulle (23 June–04 July 2004) moved northward off the eastern coast of Taiwan and made landfall at the northeastern Taiwan on 01 July, 2004 (Fig. 9a). As shown in Fig. 9b, the model meridional surface velocity (black line) in the low-velocity region reached its maximum negative value on 01 July after local wind (blue line) got its minimum strength on 29 June. Two days later, both the model (red solid line) and AVHRR–AMSR blend sea surface temperature (red dash line) reached their minima as the wind and surface flow restored to their original values. During the influence period of Mindulle, four snapshots of wind and surface flow are shown in Fig. 9c–f. Prior to the impingement of Mindulle (26 June, Fig. 9c), the Kuroshio flowed in a straight path in the Luzon Strait and the flow in the low-velocity area was northward (positive sign in warm color shading). When

Mindulle came to the vicinity of the Luzon Strait and the east coast of Taiwan (30 June, Fig. 9d), it gave rise to a northeasterly wind near the southern tip of Taiwan and a southward flow was touched off. With Mindulle moving northward, the southward flow got strongest on 01 July and weakened afterward (Fig. 9e). When Mindulle swept the sea surface around the Luzon Strait, the surface Kuroshio had a greater westward intrusion to the northern South China Sea (30 June–01 July). The flow returned to the pre-wind condition on 05 July (Fig. 9f).

The second example is concerning the impact from a distinct typhoon track. The super typhoon Haitang went from southeast to northwest, which was different from the nearly meridional path of Mindulle (2004), and made landfall at central eastern Taiwan on 18 July 2005 (Fig. 10a). As shown in Fig. 10b, the evolutions of local
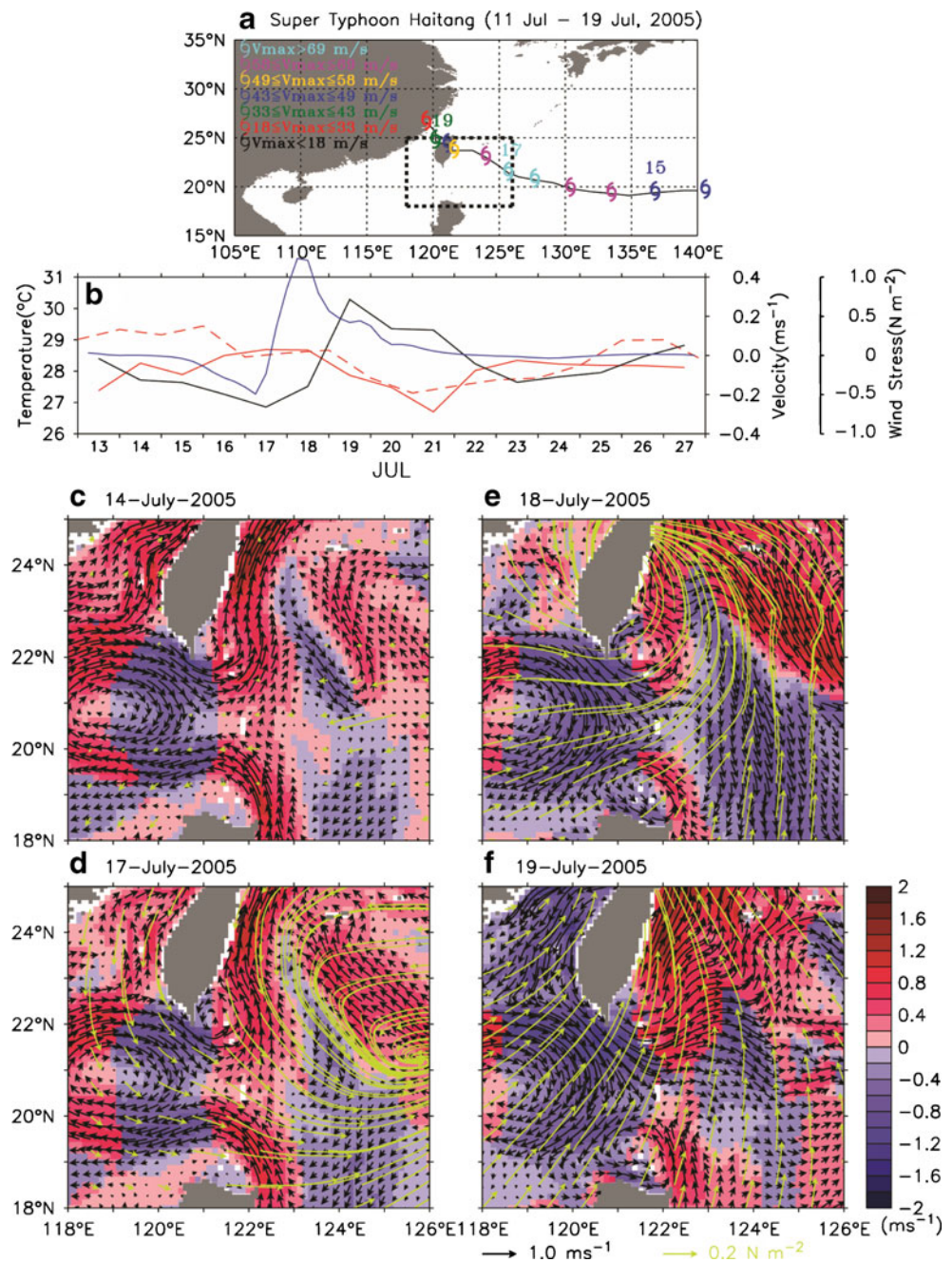
Fig. 9 **a** The track map and its related strength of super typhoon Mindulle (2004) are obtained from http://weather.unisys.com/hurricane/. **b** The AVHRR–AMSR blend SST (121° E, 22.25° N, *red dash line*), the model-derived upper-ocean temperature (0–20 m, 121° E, 22.25° N, *red solid line*), the model-derived surface meridional velocity (121° E, 22.25° N, *black line*), the meridional wind stress (121–122° E, 22–23° N, *blue line*). **c–f** Snapshots of wind stress (*green arrows*), modeled surface current (*black arrows*) and its current speed (*shading*) with the sign of meridional velocity, $\sqrt{u^2 + v^2} \times \frac{v}{|v|}$. The positive sign is for the northward flowing current

meridional wind, modeled meridional velocity, and sea surface temperature caused by Haitang are similar to those caused by Mindulle. Distinct from the pre-wind condition of Mindulle in June 2004, the surface Kuroshio formed a loop current into the northern South China Sea with a slowly southward flow in the low-velocity area, and the strength of the Kuroshio ($\sim$1.5 m s^{-1}) in 2005 (Fig. 10c) was somewhat weaker than that ($\sim$2.0 m s^{-1}) in 2004 (Fig. 9c). When Haitang approached the eastern coast of Taiwan on 17 July (Fig. 10b, d), the wind direction reversed from northwestward to southeastward, and the southward surface flow in the low-velocity

area became stronger in 17–18 July (Fig. 10d, e). With Haitang landing and passing through Taiwan, the wind turned northward again on 19 July (Fig. 10f). A few days later, the flow in the low-velocity area also revived to a weak northward current (Fig. 11c). It is noteworthy that, unlike the case of Mindulle, the surface Kuroshio east of Taiwan had an obvious alteration in this event (Fig. 9c–f). In 17–18 July, the Kuroshio east of Taiwan was invisible in the surface layer. It seems that the impact of typhoon heavily depends on the strength of the Kuroshio. When the Kuroshio is stronger as the first example above, the impact of typhoon could be much

Fig. 10 **a** The track map and its related strength of super typhoon Haitang (2005) are obtained from http://weather. unisys.com/hurricane/. **b–f** Same as the snapshots in Fig. 9, but for the period of Haitang
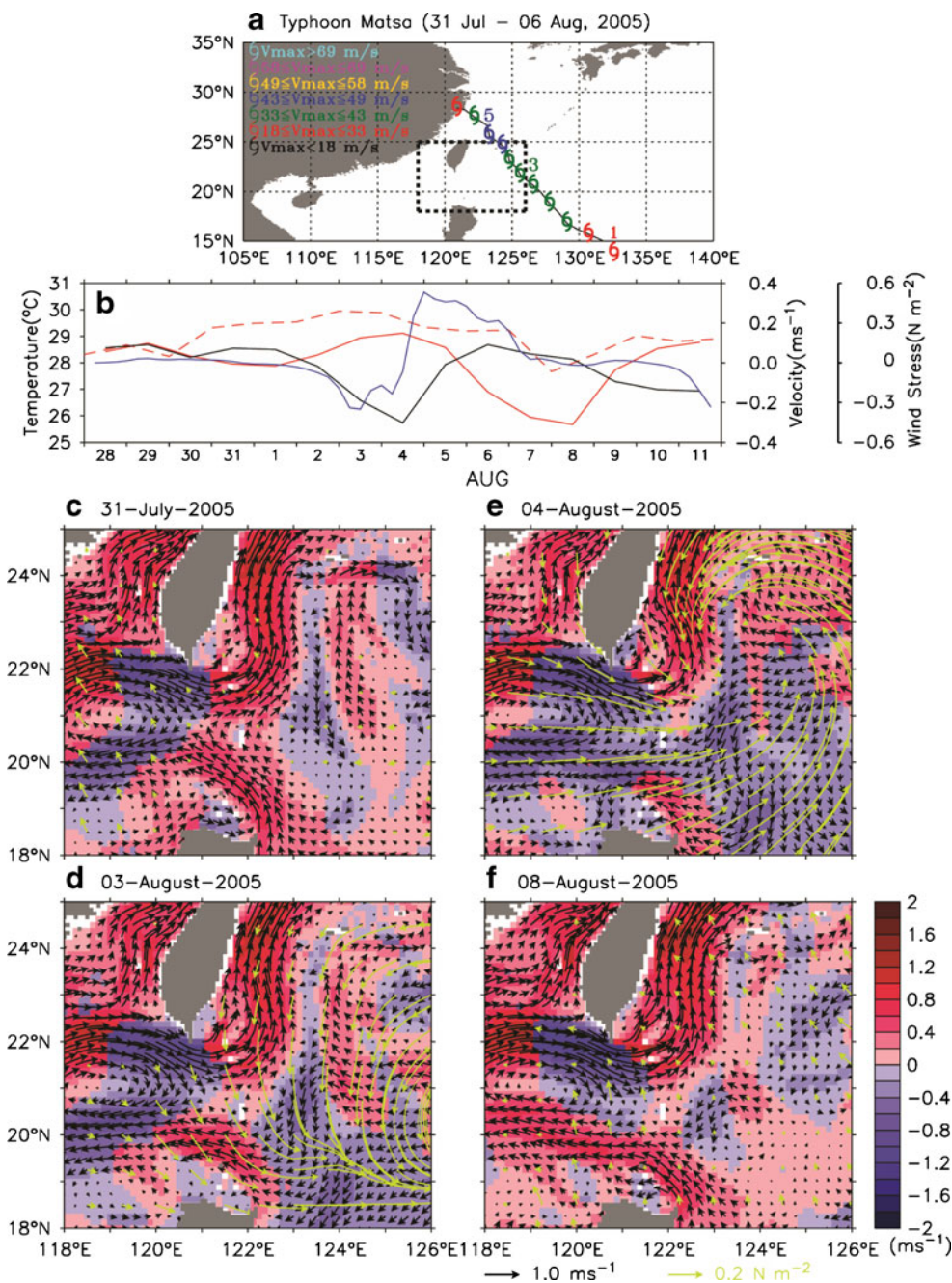

more reduced, and vice versa as the second example above.

The typhoon Matsa (2005), which is a much weaker (maximum velocity is 46 m s^{-1}) than the above two super typhoons (maximum velocities are 64 and 72 m s^{-1} for Mindulle and Haitang, respectively), is selected as the third example (Fig. 11). Matsa had a significant impact on the current east of Taiwan between 31 July and 06 August 2005. Since Matsa came just 2 weeks after Haitang left, the pre-condition of Matsa (Fig. 11c) was similar to that of Haitang (Fig. 10c). During August 03–04, when Matsa generated southward winds, the surface current in the low-velocity area had a southward velocity of as large as 0.3 m s^{-1} (Fig. 11b). In the mean time, SST dropped and reached its minimum around August 08. Unlike the case of Haitang (2005), the surface Kuroshio east of Taiwan remained visible when Matsa passed around Taiwan (Fig. 11d, e). After Matsa landed on mainland China, the current returned to the pre-typhoon condition again (Fig. 11f).

To further check the velocity variation in vertical for these cases above-mentioned, the Kuroshio core between southern Taiwan and the Lan-Yu Island located at the sea surface on the pre-typhoon condition. When the typhoon came to the neighborhood of Taiwan, the typhoon-induced

Fig. 11 a The track map and its related strength of typhoon Matsa (2005) are obtained from http://weather.unisys.com/hurricane/. b–f Same as the snapshots in Fig. 9, but for the period of Matsa

wind slowed down the surface flow and then made the Kuroshio core sink into the subsurface of about 50–100 m. Several days later, the core returned to the sea surface. To the flow below 300 m, there was a fair light impacted by the typhoon-induced wind. Furthermore, when local wind forcing was turned off in the EAMS model, the southward current and temperature drop also vanished in the low-velocity region, indicating again that typhoon-induced wind is largely responsible for the southward surface current.

Another interesting phenomenon is related to the reversal of surface current in the Taiwan Strait. Both mooring observations and numerical models have suggested that transport through the Taiwan Strait can reverse its direction when the northerly wind bursts in winter (e.g., Wu and Hsin 2005). Here, we found that southward current can also appear in the Taiwan Strait when a super typhoon sweeps around the region and inserts a large amount of southward momentum into the Taiwan Strait. Figures 10 and 11 show two examples of this. When southward wind blows, the current in the Taiwan Strait gets weaker. If this typhoon-induced wind is strong enough as in the case of Haitang (2005), the southward flow will become dominant in the Taiwan Strait. After the typhoon goes away, the

current in the Taiwan Strait will return to its normal condition to flow northeastward in only 1–2 days. Though not confirmed by observations yet, this model result raises an important issue for typhoon and coastal water interaction study, which needs to be investigated further by research.

4 Conclusions

Two significant intra-seasonal signals in the Kuroshio southeast of Taiwan are revealed by the combined use of satellite data and results from a numerical model. According to the prior studies, the cyclonic eddies originating in the interior Pacific Ocean appear to be primarily responsible for variations in the flow southeast of Taiwan at a longer time period of 30–180 days. Revealed in the study, these variations are large enough to reverse the surface flow between 122° and 123° E from a strong northward flow to a weak southward flow, but not large enough to completely diminish the intense velocity at 121.5° E, the core of the Kuroshio.

In the low-velocity region between Taiwan and the Lan-Yu Island, where the shorter period (14–28 days) fluctuations are significant, two forcing mechanisms are proposed to explain the intra-seasonal variations in summer and winter, respectively. In winter, the eastward flow, triggered by the enhanced negative wind stress curl off southwest Taiwan, produces an eastward shift of the main axis of the Kuroshio, thus weakening the current velocity in the low-velocity region. In summer, the typhoon-induced wind seems to play an important role in modulating the intensity and pathway of the surface Kuroshio southeast of Taiwan.

References

Centurioni LR, Niller PP, Lee D-K (2004) Observations of inflow of Philippine Sea surface water into the South China Sea through the Luzon Strait. J Phys Oceanogr 34:113–121

Chu T-Y (1974) The fluctuations of the Kuroshio current in the eastern sea area of Taiwan. Acta Oceanographica Taiwanica 4:1–12

Gilson J, Roemmich D (2002) Mean and temporal variability in Kuroshio geostrophic transport south of Taiwan (1993–2001). J Oceanogr 58:183–195

Hsin Y-C, Wu C-R, Shaw P-T (2008) Spatial and temporal variations of the Kuroshio East of Taiwan, 1982–2005: a numerical study. J Geophys Res 113:C04002. doi:10.1029/2007JC004485

Hwang C, Kao R (2002) TOPEX/Poseidon-derived space–time variations of the Kuroshio current: applications of a gravimetric geoid and wavelet analysis. Geophys J Int 151:835–847

Hwang C, Wu C-R, Kao R (2004) TOPEX/Poseidon observations of mesoscale eddies over the Subtropical Countercurrent: kinematic characteristics of an anticyclonic eddy and a cyclonic eddy. J Geophys Res 109:C08013. doi:10.1029/2003JC002026

Ichikawa K (2001) Variation of the Kuroshio in the Tokara Strait induced by meso-scale eddies. J Oceanogr 57:55–68

Ichikawa K, Tokeshi R, Kashima M, Sato K, Matsuoka T, Kojima S, Fujii S (2008) Kuroshio variations in the upstream region as seen by HF radar and satellite altimetry data. Int J Remote Sens 29 (21):6417–6426. doi:10.1080/01431160802175454

Jing C, Li L (2003) An initial note on quasi-stationary, cold-core Lanyu eddies southeast off Taiwan Island. Chin Sci Bull 48 (19):2101–2107

Johns WE, Lee TN, Zhang D, Zantopp R, Liu C-T, Yang Y (2001) The Kuroshio east of Taiwan: moored transport observations from WOCE PCM-1 array. J Phys Oceanogr 31:1031–1053

Kessler WS (2005) The oceans. In: Lau WKM, Waliser DE (eds) Intraseasonal variability in the atmosphere–ocean climate system. Praxis, Chichester, pp 175–212

Liang WD, Tang TY, Yang YJ, Ko MT, Chuang W-S (2003) Upper-ocean currents around Taiwan. Deep Sea Res II 50:1085–1105

Mellor GL (2004) User's guide for a three-dimensional, primitive equation, numerical ocean model, Report., 53 pp., Program in Atmos. and Oceanic Sci., Princeton Univ., Princeton

Milliff RF, Large WG, Morzel J, Danabasoglu G, Chin TM (1999) Ocean general circulation model sensitivity to forcing from scatterometer winds. J Geophys Res 104:11337–11358

Qu T, Lukas R (2003) The bifurcation of the North Equatorial current in the Pacific. J Phys Oceanogr 33:5–18

Sheu W-J, Wu C-R, Oey L-Y (2010) Blocking and westward passage of eddies in the Luzon Strait. Deep Sea Res II doi:10.1016/j.dsr2.2010.04.004

Wu C-R, Hsin Y-C (2005) Volume transport through the Taiwan Strait: a numerical study. Terrestrial, Atmospheric and Oceanic Sciences 16:377–391

Wu C-R, Chiang T-L (2007) Mesoscale eddies in the northern South China Sea. Deep Sea Res II 54:1575–1588

Wu C-R, Tang TY, Lin S-F (2005) Intra-seasonal variation in the velocity field of the northeastern South China Sea. Cont Shelf Res 25:2075–2083

Wu C-R, Lu H-F, Chao S-Y (2008) A numerical study on the formation of upwelling off northeast Taiwan. J Geophys Res 113: C08025. doi:10.1029/2007JC004697

Yang Y, Liu C-T (2003) Uncertainty reduction of estimated geo-strophic volume transports with altimeter observations east of Taiwan. J Oceanogr 59:251–257

Yang Y, Liu C-T, Hu J-H, Koga M (1999) Taiwan current (Kuroshio) and impinging eddies. J Oceanogr 55:609–617

Zhang D, Lee TN, Johns WE, Liu C-T, Zantopp R (2001) The Kuroshio east of Taiwan: modes of variability and relationship to interior ocean mesoscale eddies. J Phys Oceanogr 31:1054–1074